Mechanical Behavior of Superplastic Ultrahigh Carbon Steels at Elevated Temperature

BRUNO WALSER AND OLEG D. SHERBY

Ultrahigh carbon (UHC) steels have been investigated for their strength and ductility characteristics from 600 to 850°C. It has been shown that such UHC steels, in the carbon range 1.3 to 1.9 pct C, are superplastic when the microstructure consisted of fine equiaxed ferrite or austenite grains (~1 μm) stabilized by fine spheroidized cementite particles. The flow stress-strain-rate relations obtained at various temperatures can be quantitatively described by the additive contributions of grain boundary (superplastic) creep and slip (lattice diffusion controlled) creep. It is predicted that superplastic characteristics should be observed at normal forming rates for the UHC steels if the grain size can be stabilized at 0.4 μm. The UHC steels were found to be readily rolled or forged at high strain-rates in the warm and hot range of temperatures even in the as-cast, coarse grained, condition.

RECENTLY a class of ultrahigh carbon steels (1.3 to 1.9 pct C), combining superplastic characteristics at elevated temperature with good room temperature properties, was developed.[1-4] The basis of our ability to make plain carbon steels superplastic was the attainment of ultrafine structures with grain sizes in the order of 0.5 to 5 μm in size and cementite particles about 0.1 μm in size. The high volume fraction of cementite particles present (20 to 35 vol pct) maintains the fine grain size at warm temperature. Several thermal-mechanical processing methods were developed to obtain these fine structures.[1,2] Not only should such hypereutectoid steels exhibit superplasticity below the A_1 critical temperature, 723°C, but they should also be superplastic above the A_1 temperature. This is possible because the austenite grains obtained upon transformation should also be fine grained (since many nuclei exist from the prior fine grained ferrite). Furthermore, the fine austenite grains should remain fine because of the presence of the undissolved cementite particles. This condition should yield a wide range of temperature where superplastic flow can be expected and Fig. 1 illustrates the predicted influence of carbon on the expected range for superplastic flow. Thus, for a 1.9 pct C steel, superplasticity may be expected to be observed from 600 to 850°C, a desirable characteristic from the viewpoint of flexibility in the manipulation of temperature for superplastic metal forming.

The purpose of the present paper is to present, describe and assess the mechanical properties of ultrahigh carbon (UHC) steels (1.3 to 2.3 pct C) at elevated temperatures.

BRUNO WALSER, formerly with Department of Materials Science and Engineering, Stanford University, is now Assistant Manager, Physical Metallurgy Group, Sulzer Brothers, Winterthur, Switzerland. OLEG D. SHERBY is Professor of Materials Science and Engineering, Stanford University, Stanford, CA 94305.

Manuscript submitted December 29, 1977.

MATERIALS AND EXPERIMENTAL PROCEDURE

Castings of 1.3, 1.6, 1.9 and 2.3 pct C steels* were obtained in the form of slabs 335 mm long wherein the dimensions of the bases were 50 by 50 and 50 by 25 mm. The chemical composition of the castings is given in Table I. Examples of carbon replica transmission photographs of the as-cast microstructure are shown in Fig. 2 for a 1.6 and a 1.9 pct C steel. One observes massive primary cementite networks; oftentimes, a well developed pearlite structure is seen adjoining the proeutectoid cementite particles. The influence of extensive mechanical working on the refinement of the cast microstructure is shown in the same figure. The 1.6 pct C steel exhibits a uniformly spheroidized structure. This sample was heated to 1150°C and deformed continuously at 10 pct per pass to a true strain of about -2.0 as it cooled to 600 to 650°C; it was then isothermally rolled at 650°C, 5 pct per pass, to an additional true strain of about -1.5. The worked 1.9 pct C steel was not as fully spheroidized as the 1.6 pct C steel (lower right photograph in Fig. 2). This was, in part, attributed to insufficient

*The 2.3 pct C composition steel is more correctly defined as cast iron since most definitions place cast irons as alloys of iron and carbon containing more than 1.7 pct C. The significance of this level of carbon is that it formerly was thought to be the maximum solubility of carbon in γ-iron. In the early 1940's, however, the maximum solubility of carbon in γ-iron was shown to lie at about 2 pct and the current, widely accepted, value is 2.11 pct C.[5] Since we make only minimal reference to the 2.3 pct C composition alloy in this paper we will classify it as part of the UHC steels studied.

Table I. Chemical Composition of Ultrahigh Carbon Steels Investigated (Wt Pct)

	C	Mn	Si	P	S	Fe
1.3 pct C	1.25	0.65	0.10	0.016	0.024	bal.
1.6 pct C	1.57	0.73	0.28	0.015	0.020	bal.
1.9 pct C	1.92	0.82	0.30	0.018	0.019	bal.
2.3 pct C	2.28	0.80	0.31	0.017	0.020	bal.

ISSN 0360-2133/79/1011-1461$00.75/0
© 1979 AMERICAN SOCIETY FOR METALS AND THE METALLURGICAL SOCIETY OF AIME

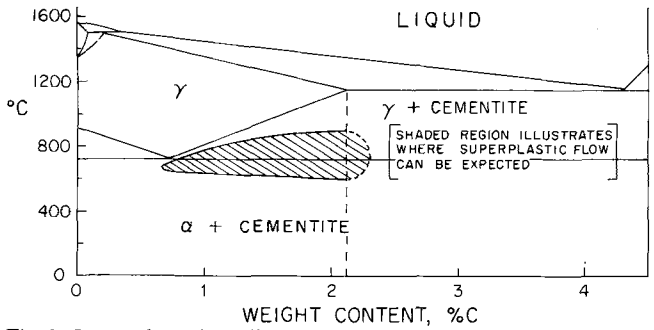

Fig. 1—Iron-carbon phase diagram illustrating range of carbon contents and temperature where superplastic flow can be expected. Fine grained hypereutectoid steels, stabilized by the presence of fine particles of cementite, can be expected to be superplastic over a wide range of temperature.

working in the alpha range (only 0.9 true strain in this case). Optical micrographs of a 1.9 pct C steel in the as-cast state and after extensive alpha working at 650°C ($\epsilon = -1.5$) are shown in Fig. 3. The grain size for a fully spheroidized steel, in the UHC steels investigated, is in the order of 0.5 to 1.5 μm and the cementite particle sizes are in the order of 0.1 to 0.5 μm. The exact grain size and carbide size depends upon the carbon content and the thermal-mechanical processing route.

Tensile specimens of rectangular cross-section were used, with a gage section of 12.7 or 25.4 mm length and different thicknesses depending on the thickness of the as-rolled plate (typically 2 to 5 mm). Transmission electron microscope specimens were

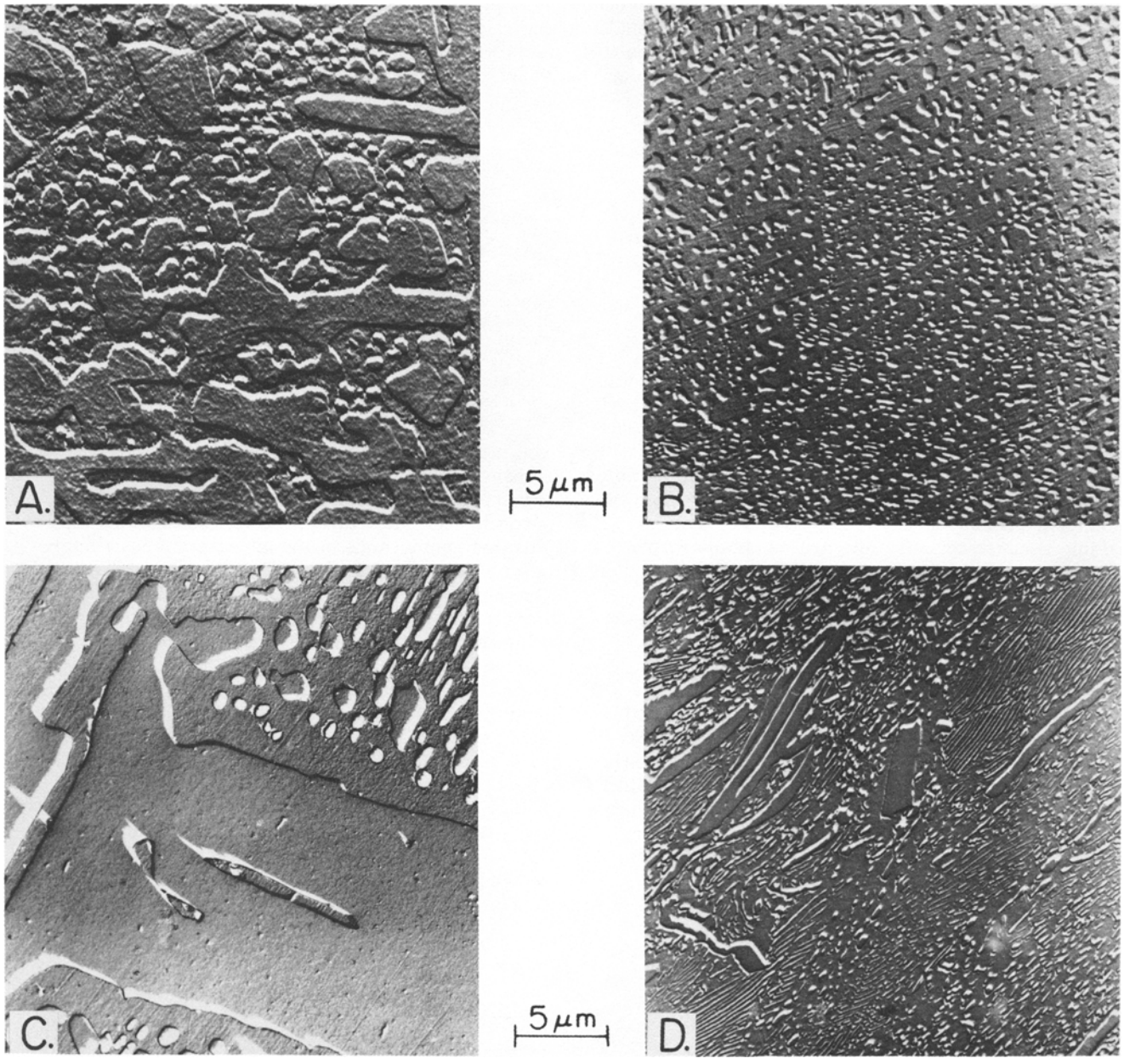

Fig. 2—The above carbon replica electron photomicrographs illustrate the influence of warm working on the breakup of the original massive cementite particles in cast ultrahigh carbon steels (left photomicrographs). Extensive warm working yielded a fully spheroidized structure in the 1.6 pct carbon steel (upper right). Considerable refinement of the structure occurred in the 1.9 pct carbon steel (lower right) by warm working but because it was not extensively worked some cementite plates are still present: (*a*) 1.6 pct carbon steel as-cast, (*b*) 1.6 pct carbon steel after warm working, (*c*) 1.9 pct carbon steel as-cast, and (*d*) 1.9 pct carbon steel after warm working.

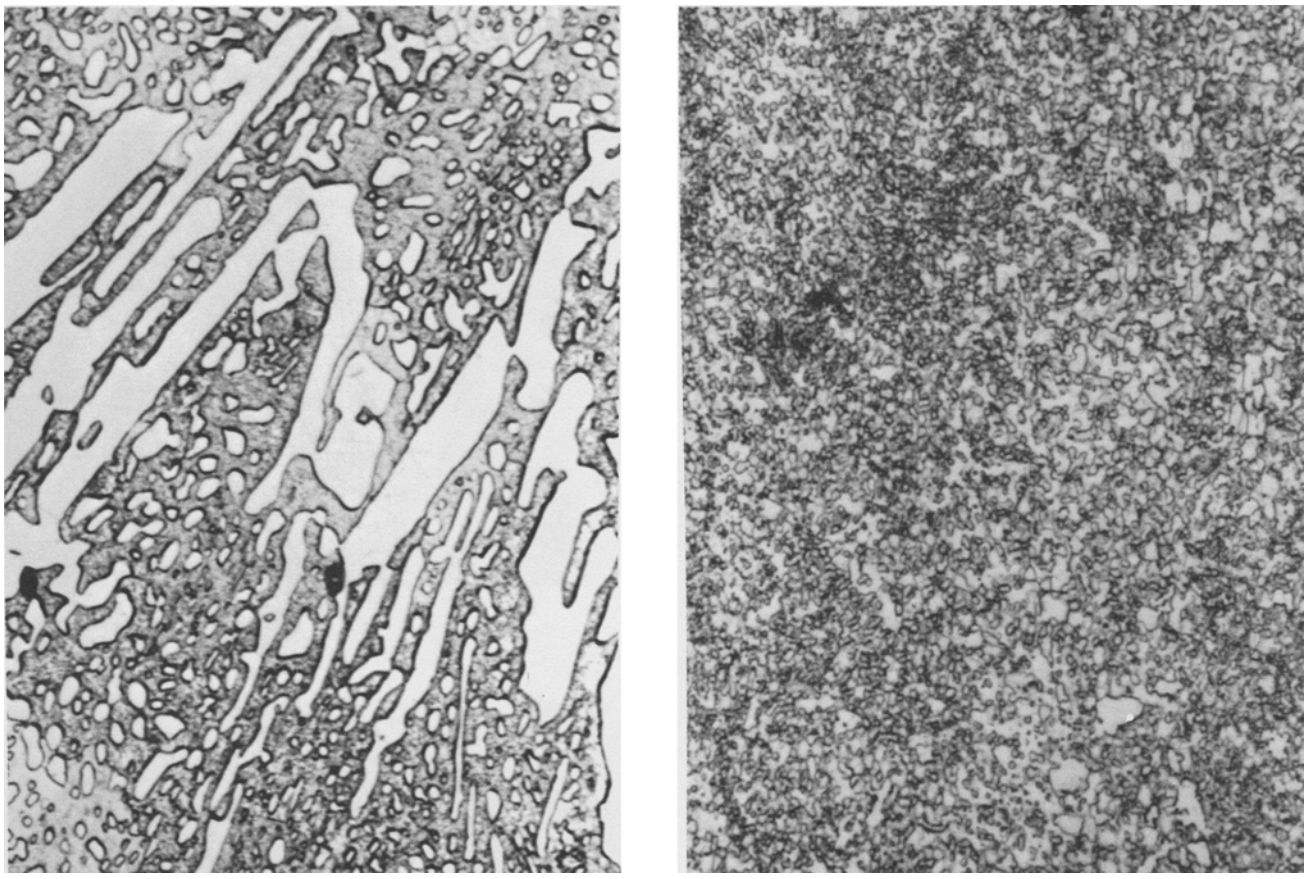

(a) (b)

Fig. 3—Optical photomicrographs of 1.9 pct C steel, illustrating change in microstructure from coarse proeutectoid cementite structure in as-cast condition (*a*) to equiaxed fine grained state in extensively hot and warm worked condition (*b*). Magnification 1674 times.

prepared by spark cutting thin plates from tested samples followed by grinding to a thickness of 0.1 mm. The final electrolytic thinning was done in an Na_2CrO_4-CH_4COOH-electrolyte at 20°C and 25 V.

RESULTS AND DISCUSSION

Most of the mechanical tests were performed in the temperature range from 600 to about 850°C where superplastic effects were noted. Three areas are discussed in the following sections; namely, the nature of the stress-strain curves observed, the flow stress-strain-rate relations noted below and above the A_1 temperature, and lastly, the influence of strain-rate and temperature on the tensile ductility.

1) Stress-Strain Curves

Examples of true stress-true strain curves obtained for the 1.6 pct C steel are shown in Fig. 4. In this figure the fully spheroidized, fine grained steel is compared with the as-cast material. The samples were deformed at an engineering strain-rate of 1 pct per min at 650°C. A high ductility (>500 pct elongation) and low flow stress of the fine grained steel compared to the coarse grained as-cast material is noted. These results follow the expected behavior, that is, fine superplastic structures exhibit lower strengths than coarse structures at elevated temperature and low strain-rates. Two results were observed, however, which were somewhat unexpected. The first relates to the considerable strain hardening that was observed to occur during superplastic flow of the fine grained steels. For example, the flow stress more than doubled (30 to 65 MPa) after 200 pct elongation. We attribute this result to grain growth that occurred

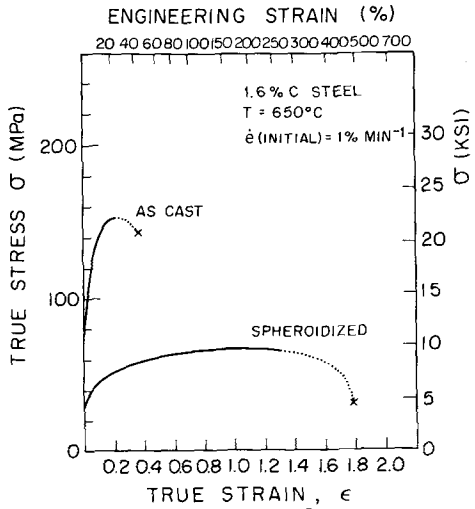

Fig. 4—True stress-true strain curves at 650°C for a 1.6 pct C steel in coarse grained, as-cast state and in spheroidized, fine grained condition.

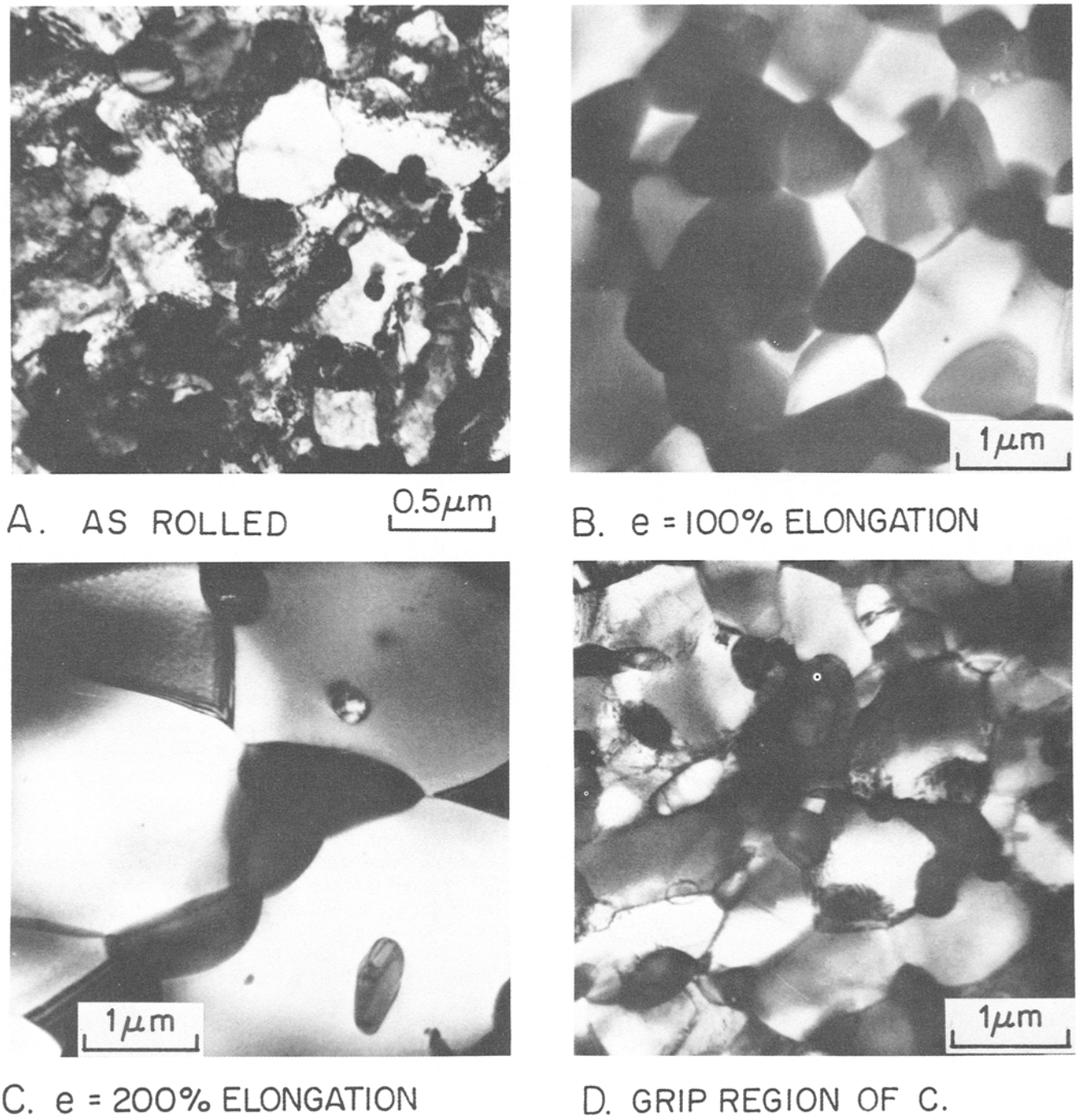

Fig. 5–Transmission electron micrographs of a warm worked 1.9 pct C steel illustrating the grain growth that occurs during superplastic flow: (*a*) steel in as-rolled condition [$(\gamma w)_C + \alpha w$ at 650°C)], (*b*) and (*c*) superplastically deformed at 650°C and $\dot{e}$ = 1 pct per min to strains indicated, (*d*) grip region of sample shown in (*c*).

during superplastic flow since it is well established that coarse grained samples are stronger than fine grained samples (typically σ is directly proportional to the grain size[6-8]). Transmission electron microscopy studies revealed that the original grain size was about 0.5 μm. After deformation to 100 pct elongation, the grain size increased to 1.5 to 2 μm and after a total elongation of 300 pct the grain size was about 3 μm. These microstructural changes during superplastic straining were typical of those noted for the 1.3, 1.6, and 1.9 pct C steels although other, less sensitive, variables were strain-rate and temperature.[4] An example of grain growth during superplastic flow of a 1.9 pct C steel is shown in the transmission photomicrographs of Fig. 5. Of special note in this figure is that straining enhances grain growth dramatically. Thus, the grip region of the tested sample (Fig. 5(*d*)), where no straining occurred, exhibits a grain size of 1 μm after exposure to the same time at temperature; this grain size is about three times smaller than that observed in the gage region of the fractured sample.

Another interesting observation in Fig. 4 is that the

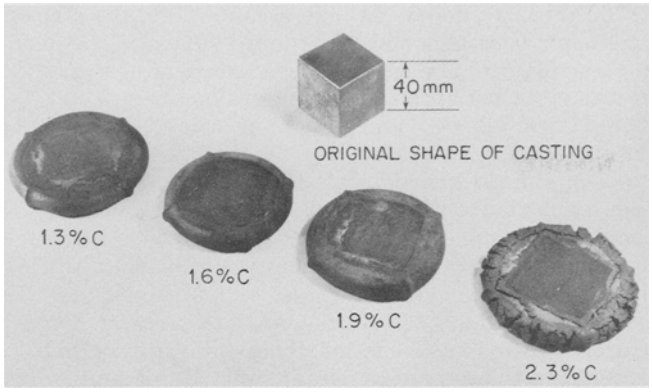

Fig. 6—The UHC steels investigated exhibit great ease of formability even in the as-cast state. The above illustrates the lack of edge cracking after one rapid forging step, to a strain of about 1.2, at 850°C. Only the 2.3 pct C steel exhibited edge cracking.

as-cast 1.6 pct C steel exhibited a respectably high elongation to fracture of 43 pct at 650°C ($T = 0.51T_m$). Such a result suggests that UHC steel castings are rather forgiving materials at elevated temperature and should not crack easily. This agreed well with our experience since edge cracking rarely occurred during rolling in the temperature range of 550 to 1100°C. An example of the forgeability of the UHC steels in the as-cast condition is shown in Fig. 6. Castings in the form of machined cubes were forged at 850°C in one step (about 3 to 5 s forging time) to the capacity of the press used, 170 tons force (1.52 MN). None of the samples exhibited cracking except the 2.3 pct C steel. The latter steel, which contains 34 vol pct cementite below the A_1 temperature, could not be worked extensively at any temperature without cracking badly. It is not at all clear why such difficulties were observed with this carbon content steel, although recent work[9] suggests that diminishing the presence of silicon may contribute to inhibition of edge cracking.

2) Change in Strain-Rate Tests

A common method of determining the flow stress-strain rate relation from a single superplastic sample is to perform strain-rate change tests.[10] This is a very convenient method and is especially meaningful when structural changes do not occur during plastic flow. This is often not the case, however, as emphasized by Rai and Grant[11] and by Baudelet and his colleagues.[12] We mentioned earlier that grain growth occurred during superplastic deformation of the ultrahigh carbon steels (Fig. 5) and that this was responsible for the strain hardening observed in the early portion of the true stress-true strain curve (Fig. 4). We developed an experimental method which helped to minimize this problem by predeforming the material to a true strain of 0.2 to 0.4 at which point a steady state flow-stress (and hence a steady state structure) was approached. The sample was then deformed small amounts at several different strain-rates. In this manner a large amount of information was obtained between the flow stress and the corresponding strain-rate over a range of strain where grain growth was minimal. The flow stress observed at each strain-rate was assumed to represent a given constant grain size (~2 μm). An example of a strain-rate change test for the 1.6 pct C steel in the gamma plus cementite range is shown in Fig. 7.

Strain-rate change tests performed at different temperatures for the 1.6 pct C steel are presented in Fig. 8 as flow stress-strain-rate curves. The influence of carbon content on the flow stress-strain-rate relation-

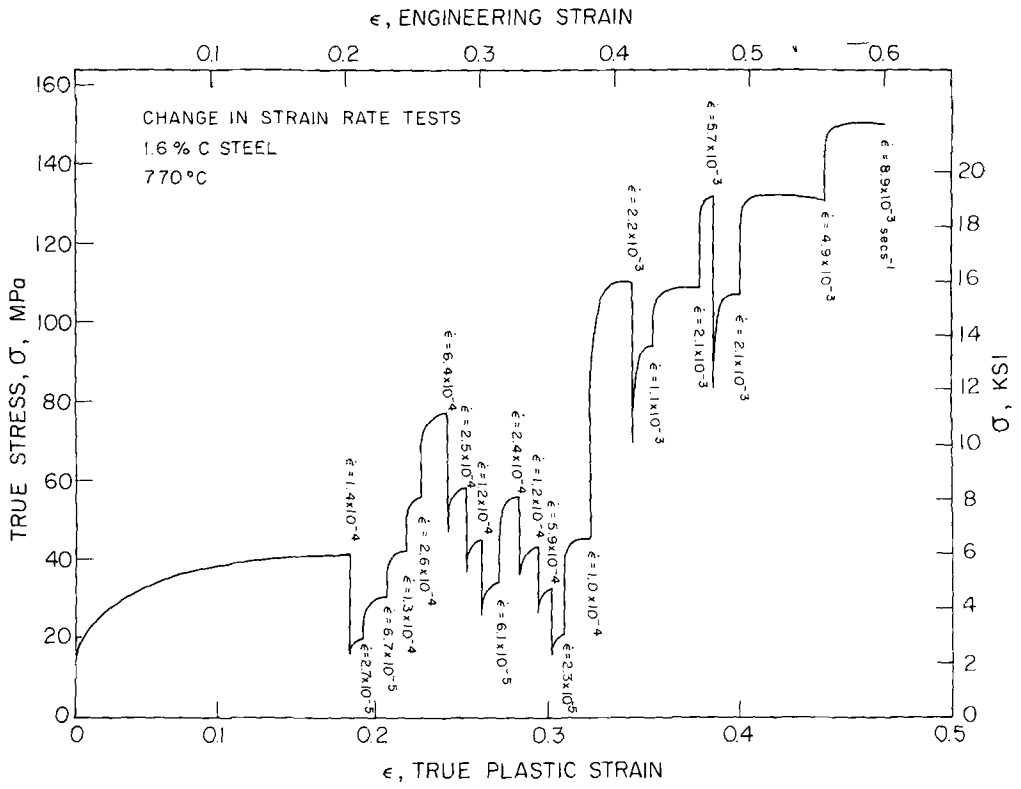

Fig. 7—This graph illustrates change in strain-rate tests performed to determine the flow stress-strain rate relation at constant structure. The example shown is for a 1.6 pct C steel tested in the austenite plus cementite range (770°C).

ship for the UHC steels is shown in Fig. 9. These data reveal the normal trend expected in superplastic materials at low strain-rates, namely the stress exponents are low and typical of those observed for superplastic metallic alloys (*i.e.* $n \simeq 2$). In this region, grain boundary sliding is believed to be the rate controlling process in plastic flow and elongations in the order of 500 to 700 pct were noted. At high strain-rates, the stress exponents were high and approached values in the order of eight (Figs. 8 and 9). [A stress exponent of eight was noted in the creep of coarse grained ($d \simeq 9$ μm) iron-carbon alloys,[13] an example of which is given in Fig. 9]. These high values can be compared with stress exponents noted in constant structure creep tests[14] at high temperature where $n = 8$. One can assume that constant structure is maintained in the UHC steel since the submicron grain size present would make it unlikely that subgrains would form and at high strain-rates virtually no grain growth occurs. In this region deformation by slip processes involving dislocation climb is believed to be the rate determining step for plastic flow.[14]

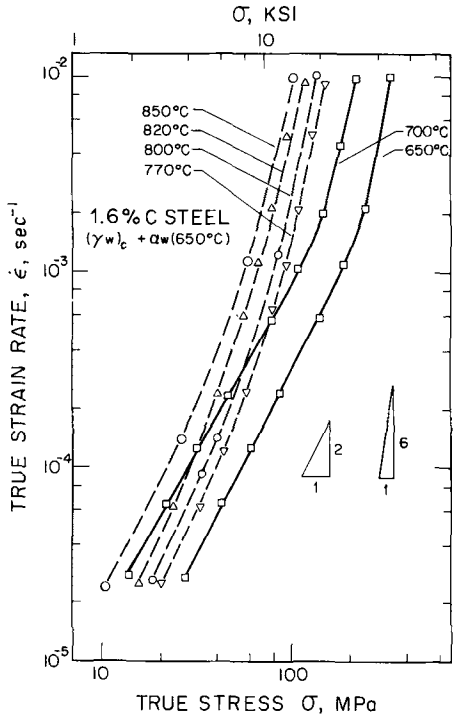

Fig. 8—Flow stress-strain rate relation for fine grained 1.6 pct C steel in the ferrite plus cementite and the austenite plus cementite temperature range.

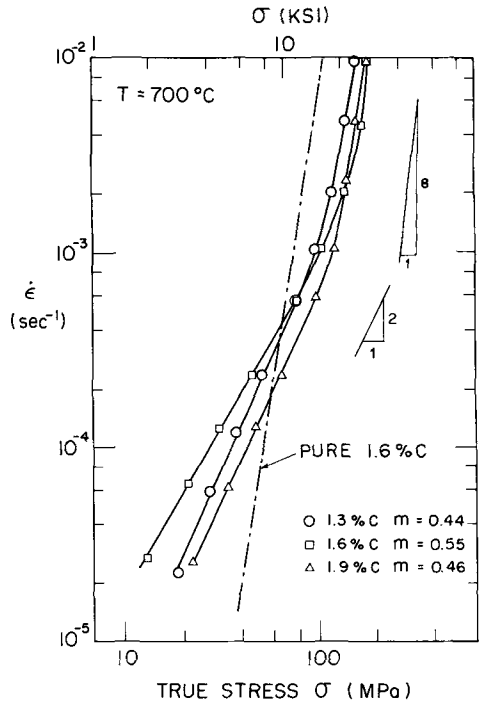

Fig. 9—Influence of carbon content on the flow stress-strain rate relationship for fine grained UHC steels at 700°C. A coarse grained ($d \cong 9$ μm) iron-carbon alloy[13] is shown for comparison where the stress exponent is seen to equal about 8.

The above results suggest that the creep-rate of the UHC steels can be correlated by means of two additive contributions to plastic flow, namely:

$$\dot{\epsilon} = \dot{\epsilon}_{sp.f.} + \dot{\epsilon}_{s.c.} \qquad [1]$$

where $\dot{\epsilon}_{sp.f.}$ is the creep-rate associated with superplastic flow and $\dot{\epsilon}_{s.c.}$ is the creep-rate associated with slip creep. Specific expressions have been developed to describe these relations. The superplastic flow rate of fine grain size materials, when grain boundary diffusion is rate controlling,[6,7,15,16] is given by:

$$\dot{\epsilon}_{sp.f.} = A \frac{\mathbf{b} D_{gb}}{d^3} \left(\frac{\sigma}{E}\right)^2 \qquad [2]$$

where $A \simeq 10^8$, d is the grain size, $\mathbf{b}$ is Burgers vector, D_{gb} is the grain boundary diffusion coefficient in the matrix phase of the superplastic material, σ is the creep stress, and E is the unrelaxed dynamic Young's modulus. The creep-rate in the slip creep range, where lattice diffusion is rate controlling is given by:[14]

$$\dot{\epsilon}_{s.c.} = A' \left(\frac{\lambda}{\mathbf{b}}\right)^3 \frac{D_L}{\mathbf{b}^2} \left(\frac{\sigma}{E}\right)^8 \qquad [3]$$

where $A' \simeq 10^9$ for high stacking fault energy materials, λ is the subgrain size or barrier spacing (in the case of the ultrahigh carbon steel the grain size or the interparticle spacing whichever is the finest), and D_L is the lattice self-diffusion coefficient.

The data shown in Fig. 8 were plotted to determine the activation energy for plastic flow in the two regions in order to compare the results with those predicted by Eqs. [2] and [3]. The method selected to calculate the activation energy was to plot the modulus compensated flow stress *vs* the reciprocal absolute temperature. This permitted using data within the superplastic region and within the slip creep region. Thus, the activation energy for plastic flow, from Eqs. [2] and [3], can be calculated by:

$$Q\Big|_{\dot{\epsilon} = \text{constant}} = \frac{R \, d \ln \left(\frac{\sigma}{E}\right)^n}{d \, 1/T} \qquad [4]$$

Plots for determination of the activation energy are given in Fig. 10(*a*) and (*b*). As can be seen, the activation energy for plastic flow in the superplastic region (Fig. 10(*b*)) is about 160 kJ/mol in both the alpha and gamma plus cementite region; these values are nearly identical to the grain boundary self diffusion activation

Table II. Grain Boundary, Lattice Diffusion and Modulus Data for Iron in the Ferrite and Austenite Phase Regions

	Grain Boundary Diffusion*			Lattice Diffusion†			Elastic Modulus
T, °C	D_o, 10^{-4} m²/s	Q, kJ/mol	D_{gb}, m²/s	D_o, 10^{-4} m²/s	Q, kJ/mol	D_L, m²/s	$E^{(G)}$, MPa
Alpha iron + Fe_3C	17.7	170		1.6	252		
650			4.1×10^{-13}			9.0×10^{-19}	1.61×10^5
700			1.3×10^{-12}			5×10^{-18}	1.52×10^5
Gamma iron + Fe_3C	1.8	163		0.18	270		
770			1.2×10^{-12}			4×10^{-18}‡	1.35×10^5

*Average values, based on Refs. A, B, and C.

†Average values taken from a number of sources quoted in Ref. (D).

‡Extrapolation of pure gamma iron data ($T > 910$°C) down to 770°C, then multiply by seven because of the enhancement of gamma iron self diffusion by carbon in solution at 770°C (0.8 wt pct C) as determined from Refs. E and F.

References for Table II.

(A) C. Leymonie, Y. Adda, A. Kirianenko, P. LaCombe, Compt. Rend. *248*, (1959) 1512.
(B) D. W. James, G. H. Leak, Phil. Mag., *12*, (1965) 491.
(C) P. LaCombe, P. Guiraldeng, C. Leymonie, *Radioisotopes in the Physical Science Industry*, (1962) I.A.E.A. Vienna, 179.
(D) O. D. Sherby, P. M. Burke, Progr. Mater. Sci., *13*, (1967) 333.
(E) P. L. Gruzin, R. V. Kornev, G. V. Kurdimov, Dokl. Acad. Nauk., USSR, *80* (1957) 49.
(F) H. W. Mead, C. E. Birchenall, Trans. AIME, *206* (1956) 1336.
(G) W. Koster, Z. fur Metallkde, *39*, (1948) 1.

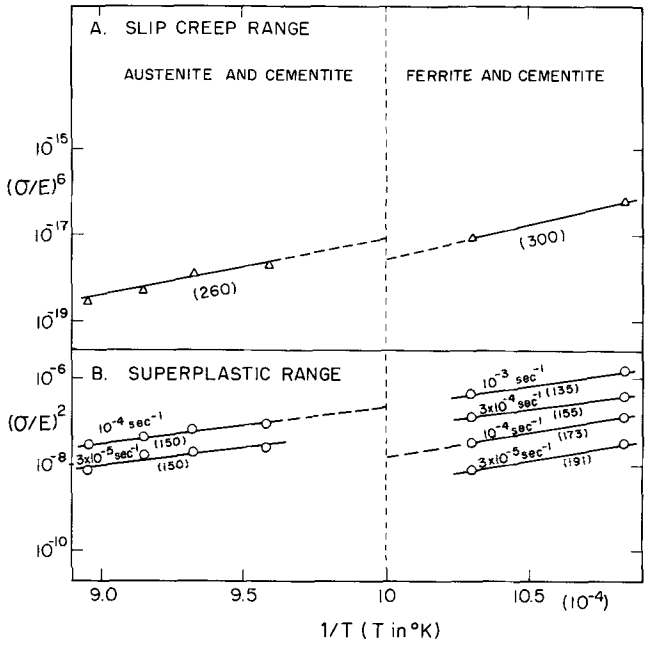

Fig. 10—Activation energy for plastic flow calculated from plots of modulus compensated stress as a function of reciprocal absolute temperature. Values of activation energy are given in parenthesis (kJ/mol) in the slip creep range and in the superplastic range.

energy of iron in alpha iron, 170 kJ/mol, and in gamma iron, 163 kJ/mol (Table II).

The activation energy for plastic flow in the slip creep region was more difficult to determine with the available data. This is because the stress exponent, n, at high stresses was not eight but rather more nearly six (Fig. 8). We hypothesize that this is because the slip creep process is not yet fully rate controlling at the highest strain-rates investigated. Using $n = 6$, the activation energy for plastic flow in the slip creep region (Fig. 10(a)) was determined to be about 280 kJ/mol. This value correlates quite well with the activation energy for creep of coarse grained ultrahigh carbon-iron alloys[13] where $Q = 250$ kJ/mol; in this case, $n = 8$ over a wide range of stress (see dashed line in Fig. 8). These values for plastic flow in the slip creep region are essentially equal to the activation energy for lattice diffusion in alpha iron (251 kJ/mol) and in gamma iron (270 kJ/mol) (Table II).

The above calculations yield qualitative evidence that the UHC steels behave in a manner predicted by the phenomenological creep flow Eqs. [2] and [3]. More importantly, a quantitative prediction can be made. Thus, the creep behavior of the 1.6 pct C steel in the alpha plus cementite region can be predicted by Eqs. [2] and [3] since D_{gb} and D_L are known for alpha iron (Table II) and since the grain size, d, and the barrier

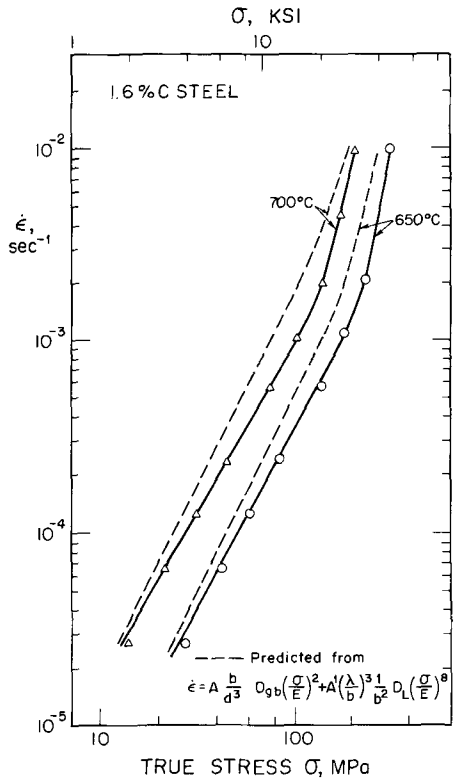

Fig. 11—The flow stress-strain rate relationship for fine grained 1.6 pct C steel is compared with that predicted from the additive contribution of slip creep and superplastic creep [Eqs. [2] and [3]]. Burgers vector was assumed equal to 2.5Å.

spacing, λ, are known after plastic flow in this region. As mentioned previously, grain growth occurred due to the superimposed effect of strain and time during superplastic flow; grain sizes in the superplastically deformed samples were typically 2 μm in the range of strains where strain rate change tests were performed to obtain the data given in Fig. 8 and Fig. 9. To compare the experimental flow stress-strain-rate data with Eqs. [2] and [3], the grain size, d, was chosen as 2 μm to substitute into the superplastic flow rate expression and λ = 0.5 μm was chosen for the slip creep flow rate expression (the interparticle spacing was taken as the barrier spacing). The result of the prediction is shown in Fig. 11 for the 1.6 pct C steel at 650 and 700°C. As can be seen, good quantitative correlations were obtained, attesting to the probable validity of the superplastic flow and slip creep relations in describing the creep behavior of fine grain size ultrahigh carbon steels.

The strength difference of the 1.6 pct C steel above and below the A_1 is readily seen in Fig. 10. Extrapolation of the data in this figure to the transition temperature reveals that the UHC steel in the gamma plus cementite region is stronger than in the alpha plus cementite region. This is probably due to the lower diffusion rate in the fcc austenitic steel than in the ferritic steel. It was decided to compare the stress-strain-rate relation for the UHC steel both above and below the A_1 by selecting a temperature at which the grain boundary diffusion coefficients were identical. The two temperatures selected were 700°C for the alpha plus cementite range and 770°C for the gamma plus cementite range. At these temperatures, $D_{gb} \simeq 1.2 \times 10^{-12}$ m^2/s (Table II). By coincidence, the lattice self diffusion coefficients in the ferritic and austenitic phases were also nearly identical, $D_L \simeq 5 \times 10^{-18}$ m^2/s (Table II). And, the dynamic Young's modulus values for pure iron in the two crystalline forms are also quite similar, $(E_\gamma)_{770°C} = 1.35 \times 10^5$ MPa and $(E_\alpha)_{770°C} = 1.52 \times 10^5$ MPa. (The modulus value for gamma iron at 770°C should be corrected for the 0.9 wt pct C in solution at this temperature; no modulus data appear available to make the appropriate calculation, although the correction is likely to be small.) A comparison of the 1.6 pct C steel at 700 and 770°C is shown in Fig. 12. The curves nearly superimpose attesting to the previous suggestion that the appropriate diffusion coefficients (D_{gb} and D_L) and the elastic moduli properly account for the plastic flow behavior of the 1.6 pct C steel. In the following we will discuss the possible reasons for the minor differences noted in the two curves. At low strain-rates, the austenitic phase material is slightly stronger than the ferritic phase material in the superplastic region; this can be attributed to a grain size difference since grain growth is likely to be enhanced in the austenite region because there is less cementite present than in the ferrite region (12.5 vol pct Fe_3C at 770°C compared to 25 vol pct Fe_3C at 700°C). At high strain-rates in the slip creep region, the ferritic phase material is stronger than the austenitic phase material. Several factors can contribute to the latter observation. First, the barrier spacing (*i.e.* the interparticle spacing and the grain size) in the ferrite range is probably smaller than in the austenite range; if Eq. [3] is used to predict the difference in barrier spacing from the difference in strength, about a factor of two is calculated. We believe this to be the most likely factor influencing the difference in strength at high strain-rates. A second factor is that solid solution hardening (*e.g.* atom size differences) from the presence of manganese and silicon may be more effective in the ferritic than in the austenitic phase. And, a third factor is the possible contribution of the hardness of cementite per se to the strength of the iron-cementite composite that makes up the 1.6 pct C steel studied. That is, it is known[17] that the hardness of cementite is an order of magnitude higher than the hardness of alpha iron at 700°C but is only a factor of two harder than gamma iron when the hardness data are extrapolated to 770°C.

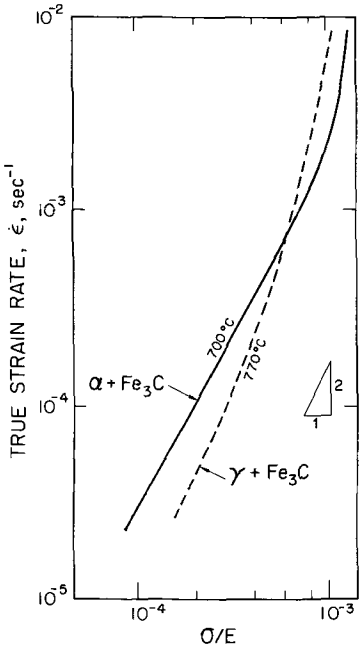

Fig. 12—The modulus compensated flow stress-strain rate relationship for 1.6 pct C steel is compared at 770°C (austenite plus cementite range) and at 700°C (ferrite plus cementite range) where the diffusion coefficients are nearly identical. The small difference in the resulting curves can be primarily attributed to a difference in grain size.

3) Influence of Strain-Rate and Temperature on the Tensile Ductility

The above discussion reveals that UHC steels when in fine grained form exhibit all the characteristics expected of a superplastic material. The tensile ductility increased in value as the strain-rate sensitivity exponent, m, increased, following the usual trends described extensively in the literature.[18,19] The results of isostrain-rate tests performed to determine the tensile elongation are given in Table III. These tabulated data are plotted in Fig. 13 as tensile ductility against the diffusion compensated strain-rate. Elongations to failure of as high as 750 pct were obtained for the UHC steels when the strain-rate sensitivity exponents reached values of 0.5. Samples tested in the ferrite plus cementite range exhibited higher elongations, as an average, than samples in the austenite plus cementite range. This difference is attributed to the slightly coarser grain size that may exist in the austenite range compared to that in the ferrite range. All samples exhibited necking prior to failure; the

fracture region, however, never exhibited a chisel point failure (*i.e.* reduction of area was less than 100 pct). This was rather surprising since no evidence of cracking was observed in the UHC steels in regions away from the fractured region. Regions adjoining the fracture surface, however, exhibited the presence of minute voids mostly at interphase boundary sites.*

*Recent investigations[20,21] have revealed that appropriate control of chemical composition (primarily low silicon content and small additions of carbide stabilizing elements like chromium) can lead to tensile elongations exceeding 1500 pct and to chisel point type fractures (100 pct R.A.).

The UHC steels studied in this investigation are superplastic up to strain-rates of as high as 10 pct per min (Table III and Fig. 13). Although these are respectably high strain-rates, they are not in the order of commercial forming rates. From a practical and economical point of view it would be highly desirable if the UHC steels could be superplastic at normal forming rates, *i.e.* 10^{-1} to 1 s^{-1} (600 to 6000 pct per min). Such a goal is a realistic one and the principal method of achieving it is to develop a grain size finer than one micron in size which remains stable during superplastic flow. This concept is illustrated graphically in Fig. 14, utilizing Eqs. [2] and [3] to make the predictions. In this figure the strain-rate stress relation for our 1.6 pct C steel deformed at 700°C is shown. As mentioned previously the average grain size of this steel during superplastic flow is 2 μm. If the grain size is decreased by a factor of five, that is, to a size of 0.4 μm, the superplastic flow rate, at a given stress, is enhanced by over a hundred fold ($5^3 = 125$). The resulting strain-rate stress relation for the 0.4 μm grain size steel, shown in Fig. 14, is such that superplastic flow now extends to a strain-rate of about 1 per s. It is clear that optimization of the maximum superplastic flow rate is desirable. Currently an attempt is being made to control the stability of the fine grain size through chemical composition. The in-

Table III. Elongations to Fracture for the Superplastic Ultrahigh Carbon Steels Under Different Test Conditions*

Test No.	Material and Alpha Working, α_w, History	Test T, °C	Initial Strain-Rate $\dot{\epsilon}$, Pct min^{-1}	$\dot{\epsilon}$, s^{-1}	$\dot{\epsilon}/D_{gb}$, m^{-2}	Elongation to Fracture, Pct
1	1.3 pct C $\alpha_w(650)\ \epsilon_\alpha = 1.7$	605	1	1.7×10^{-4}	2.2×10^{2}	230
2	$\alpha_w(650)\ \epsilon_\alpha = 1.2$	630	0.8	1.3×10^{-4}	4.85×10^{0}	700
3	$\alpha_w(650)\ \epsilon_\alpha = 1.2$	650	0.8	1.3×10^{-4}	3.17×10^{0}	600
4	$\alpha_w(650)\ \epsilon_\alpha = 1.2$	650	1	1.7×10^{-4}	4.15×10^{0}	480
5	$\alpha_w(650)\ \epsilon_\alpha = 1.2$	650	1	1.7×10^{-4}	4.15×10^{0}	250
6	$\alpha_w(565)\ \epsilon_\alpha = 1.7$	650	10	1.7×10^{-3}	4.15×10^{1}	320
7	$\alpha_w(565)\ \epsilon_\alpha = 0.8$	650	100	1.7×10^{-2}	4.15×10^{2}	76
8	$\alpha_w(565)\ \epsilon_\alpha = 1.7$	800	10	1.7×10^{-3}	7.94×10^{0}	140
9	1.6 pct C $\alpha_w(565)\ \epsilon_\alpha = 1.5$	600	10	1.7×10^{-3}	1.38×10^{2}	207
10	$\alpha_w(650)\ \epsilon_\alpha = 1.7$	620	0.4	6.7×10^{-5}	3.22×10^{0}	489
11	$\alpha_w(650)\ \epsilon_\alpha = 1.7$	630	0.8	1.3×10^{-4}	4.85×10^{0}	760
12	$\alpha_w(650)\ \epsilon_\alpha = 1.7$	650	0.4	6.7×10^{-5}	1.63×10^{0}	473
13	$\alpha_w(650)\ \epsilon_\alpha = 1.7$	650	1	1.7×10^{-4}	4.15×10^{0}	486
14	$\alpha_w(565)\ \epsilon_\alpha = 1.0$	650	1	1.7×10^{-4}	4.15×10^{0}	334
	as cast	650	1	1.7×10^{-4}		43
16	$\alpha_w(650)\ \epsilon_\alpha = 1.7$	650	4	6.7×10^{-4}	1.63×10^{1}	532
17	$\alpha_w(650)\ \epsilon_\alpha = 1.7$	650	10	1.7×10^{-3}	4.15×10^{1}	457
18	$\alpha_w(500)$ + 100 h /500°C $\epsilon_\alpha = 1.7$	650	10	1.7×10^{-3}	4.15×10^{1}	273
19	$\alpha_w(565)\ \epsilon_\alpha = 1.0$	650	10	1.7×10^{-3}	4.15×10^{1}	270
20	$\alpha_w(700)$ + 100 h /500°C $\epsilon_\alpha = 1.3$	650	10	1.7×10^{-3}	4.15×10^{1}	240
21	$\alpha_w(650)\ \epsilon_\alpha = 1.1$	650	100	1.7×10^{-2}	4.15×10^{2}	78
22	$\alpha_w(650)\ \epsilon_\alpha = 1.7$	670	0.4	6.7×10^{-5}	9.6×10^{-1}	361
23	$\alpha_w(650)\ \epsilon_\alpha = 1.1$	700	10	1.7×10^{-3}	1.3×10^{1}	262
24	no α_w	700	10	1.7×10^{-3}		73
25	$\alpha_w(565)\ \epsilon_\alpha = 1.0$	750	200	3.3×10^{-2}	3.75×10^{2}	83
26	$\alpha_w(650)\ \epsilon_\alpha = 1.7$	770	1	1.7×10^{-4}	1.41×10^{0}	421
27	$\alpha_w(650)\ \epsilon_\alpha = 1.8$	770	1	1.7×10^{-4}	1.41×10^{0}	165
28	$\alpha_w(650)\ \epsilon_\alpha = 1.8$	770	10	1.7×10^{-3}	1.41×10^{1}	183
29	$\alpha_w(650)\ \epsilon_\alpha = 1.8$	770	100	1.7×10^{-2}	1.41×10^{2}	89
30	$\alpha_w(565)\ \epsilon_\alpha = 1.5$	800	1	1.7×10^{-4}	7.93×10^{-1}	234
31	$\alpha_w(565)\ \epsilon_\alpha = 1.5$	800	10	1.7×10^{-3}	7.93×10^{0}	397
32	no α_w	800	10	1.7×10^{-3}	7.93×10^{0}	120
33	$\alpha_w(565)\ \epsilon_\alpha = 1.5$	800	100	1.7×10^{-2}	7.93×10^{1}	165
	1.9 pct C $\alpha_w(650)\ \epsilon_\alpha = 0.9$					
34	+700°C/30 min	650	1	1.7×10^{-4}	4.15×10^{0}	378/380
35	$\alpha_w(565)\ \epsilon_\alpha = 0.2$	650	1	1.7×10^{-4}	4.15×10^{0}	231
36	$\alpha_w(565)\ \epsilon_\alpha = 1$	650	1	1.7×10^{-4}	4.15×10^{0}	334
37	$\alpha_w(593)\ \epsilon_\alpha = 1.1$	650	1	1.7×10^{-4}	4.15×10^{0}	328
38	$\alpha_w(650)\ \epsilon_\alpha = 0.9$ +700°C/30 min	700	10	1.7×10^{-3}	1.3×10^{1}	222
39	same	650	10	1.7×10^{-3}	4.15×10^{1}	254
40	same	770	10	1.7×10^{-3}	1.41×10^{1}	195

*All ultrahigh carbon steels were first worked by continuous rolling from an initial temperature of 1200°C to a final temperature of 650°C achieving a total true strain of about two. The subsequent alpha working treatment, α_w, is described in the table and the true strain, ϵ_α, introduced during work in the $\alpha + Fe_3C$ region is listed.

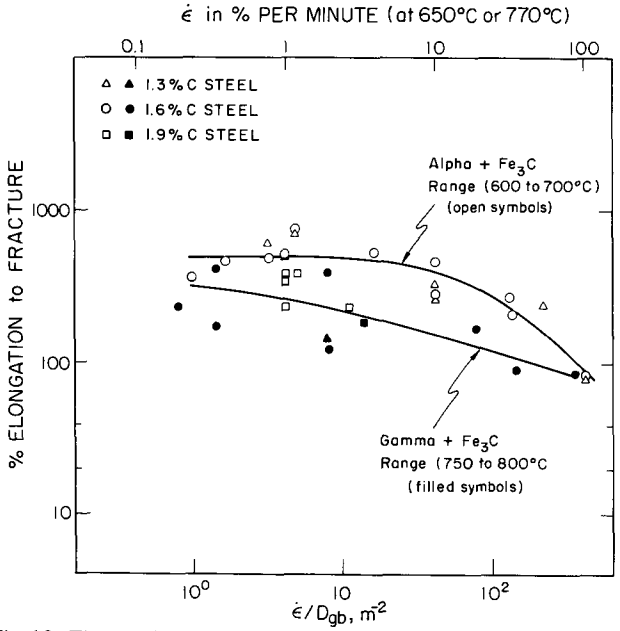

Fig. 13—The tensile ductility is plotted as a function of the grain boundary diffusion compensated strain-rate for several fine grained UHC steels.

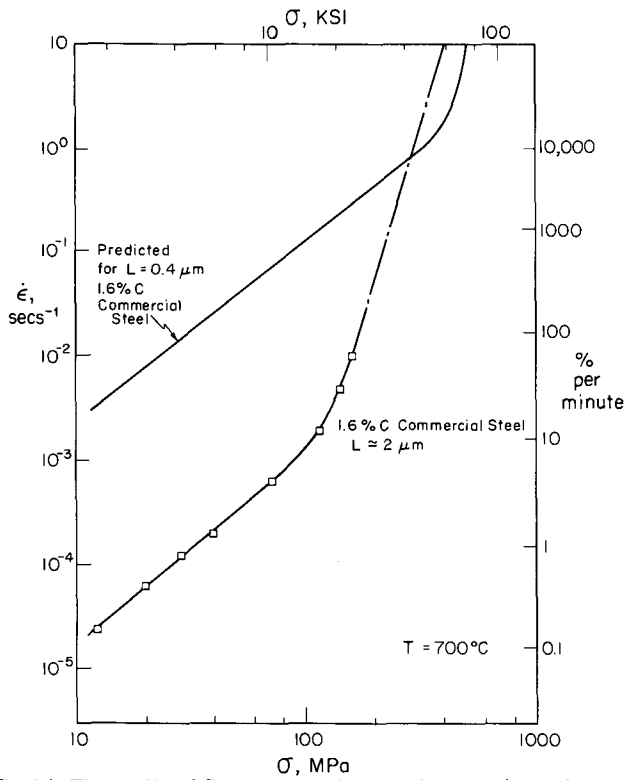

Fig. 14—The predicted flow stress-strain rate relation is shown for a 1.6 pct C steel for a stable grain size of 0.4 μm at 700°C. Under these conditions superplastic flow should be observed at strain-rates as high as one per s.

fluence of a variety of steel making or alloying elements has been assessed. These include Ni and V,[20] Cr,[21] and Mn, Si, Ti and P.[22]

SUMMARY AND CONCLUSIONS

The superplastic properties of ultrahigh carbon (UHC) steels (1.3 to 1.9 pct C) have been investigated in the ferrite plus cementite as well as the austenite plus cementite ranges of temperature, *i.e.* 600 to 850°C. The following characteristics were noted:

1) The UHC steels exhibited strain hardening during superplastic flow at all temperatures of testing. This was attributed to grain coarsening during superplastic straining. For example, the ferrite grain size increased from 0.5 to about 2.0 μm during superplastic deformation at 650°C, although it remained remarkably stable at 650°C if there was no concurrent deformation.

2) At low strain-rates, the stress exponent, n, in the equation $\dot{\epsilon} \propto \sigma^n$, was observed to be about two, a value generally attributed to superplastic flow by grain boundary sliding. At high strain-rates, the stress exponent was observed to approach eight, a value attributed to plastic flow by a slip creep mechanism where grain boundaries and cementite particles are considered as barriers to plastic flow.

3) In the range where superplastic flow dominates, the activation energy was found equal to about 170 kJ/mol a value nearly equal to that for grain boundary self-diffusion in alpha or gamma iron. In the range where slip creep dominates, the activation energy was found to be considerably higher than 170 kJ/mol and was identified with the activation energy for lattice self-diffusion in alpha or gamma iron.

4) The tensile ductility was high at low values of the diffusion compensated strain-rate, with elongations to failure in the range 300 to 750 pct. The tensile ductility was higher below the A_1 temperature (ferrite plus cementite range) than above the A_1 temperature (austenite plus cementite range). This was attributed to the lower content of cementite above the A_1 than below the A_1 leading to enhanced grain growth in the austenite plus cementite range.

5) The UHC steels exhibited high ductility at warm and hot temperatures even in the as-cast, coarse structure state. No edge cracking was noted in large strain forging experiments on the as-cast carbon steels even at temperatures as low as 850°C. These results suggest that such UHC steels have a wide range of workability.

ACKNOWLEDGMENTS

The authors wish to acknowledge support of the Defense Advanced Research Projects Agency and the Office of Naval Research in this program of research. They are especially grateful to Drs. E. Van Reuth, A. Bement, and B. A. MacDonald for their guidance and cooperation. All of our thermal-mechanical processing was done at the Lockheed Palo Alto Laboratories, and we gratefully acknowledge Mr. Roger Perkins and Dr. Thomas E. Tietz for permission to use this facility. Thanks are also extended to Dr. J. Wadsworth for his assistance in various phases of the work on the ultrahigh carbon steels. One of the authors (B.W.) would like to thank the Swiss Federal Institute of Technology (ETH-Zurich), especially to Professor Dr. W. Epprecht, for support.

REFERENCES

1. O. D. Sherby, B. Walser, C. M. Young, and E. M. Cady: *Scr. Met.*, 1975, vol. 9, p. 569.
2. U.S. Patent No. 3,951,697, issued April 20, 1976.

3. Bruno Walser, E. Sabri Kayali, and Oleg D. Sherby: *Fourth International Conference on the Strength of Metals and Alloys,* Conference Proceedings, vol. 1, pp. 456-60, Nancy, France, 1976.
4. Bruno Walser and Oleg D. Sherby: Second Annual Technical Report, Defense Advanced Research Projects Agency, Washington, D.C., Grant No. DAHC-14-73-G15, July 1, 1974-June 30, 1976.
5. Metals Handbook, Eighth Edition, vol. 8, p. 275, ASM, Metals Park, OH, 1973.
6. C. M. Packer and O. D. Sherby: *Trans. ASM,* 1967, vol. 60, p. 21.
7. J. E. Bird, A. K. Mukherjee, and J. E. Dorn: *Quantitative Relation between Properties and Microstructure,* D. G. Brandon and A. Rosen, eds., p. 255, Israel University Press, 1969.
8. J. W. Edington, K. N. Melton, and C. P. Cutler: *Progr. Mater. Sci.,* 1976, vol. 21, p. 61.
9. J. Wadsworth, L. E. Eiselstein, and O. D. Sherby: *Mater. Eng. Appl.,* 1979, vol. 1, p. 143.
10. W. A. Backofen, J. R. Turner, and D. H. Avery: *Trans. ASM,* 1964, vol. 57, p. 980.
11. G. Rai and N. J. Grant: *Met. Trans. A,* 1975, vol. 6A, p. 385.
12. B. Baudelet: *Fourth International Conference on the Strength of Metals and Alloys,* Conference Proceedings, vol. 1, pp. 2-25, Nancy, France, 1976.
13. S. Kayali: Ph.D. Dissertation, Stanford University, CA, July 1976.
14. O. D. Sherby, R. H. Klundt, and A. K. Miller: *Met. Trans. A,* 1977, vol. 8A, p. 843.
15. Richard A. White: Ph.D. Dissertation, Stanford University, CA, March 1978.
16. O. D. Sherby, R. D. Caligiuri, E. S. Kayali, and R. A. White: *Recent Advances in Metals Processing,* J. J. Burke, V. Weiss, and R. Mehrabian, eds., Twenty-Fifth Sagamore Army Materials Research Conference, Syracuse Press, NY, in press, 1979.
17. K. G. Gove and J. A. Charles: *Met. Technol.,* 1974, vol. 1, p. 229.
18. D. A. Woodford: *Trans. ASM,* 1969, vol. 62, p. 291.
19. W. B. Morrison: *Trans. ASM,* 1968, vol. 61, p. 423.
20. J. Wadsworth and O. D. Sherby: *J. Mech. Work Technol.,* 1978, vol. 2, p. 53.
21. J. Wadsworth and O. D. Sherby: *J. Mater. Sci.,* 1978, vol. 13, p. 2645.
22. T. Oyama, J. Wadsworth, M. Korchynsky, and O. D. Sherby: *Fifth International Conference on the Strength of Metals and Alloys,* Conference Proceedings, Aachen, Germany, Pergamon Press, in press, August 1979.